



International Conference on Analytical Models and New Concepts in Concrete and Masonry Structures AMCM'2017

## Bond behavior of GRFP bars to concrete in beam test

Renata Kotynia<sup>a,\*</sup>, Damian Szczech<sup>a</sup>, Monika Kaszubska<sup>a</sup>

<sup>a</sup>Lodz University of Technology, Al. Politechniki 6, 90-924 Lodz, Poland

---

### Abstract

Bond behavior between reinforcing bars and concrete is a key problem to understand behavior of reinforced concrete members. The introduction of the new reinforcing system made of fiber reinforced polymer (FRP) to construction industry forced the study of FRP-to-concrete bond behavior as one of the main mechanical properties. The application of FRP reinforcement in concrete structures increased rapidly in last years. Their excellent corrosion resistance, high tensile strength, good non-magnetic properties were the reason why they have become an alternative to traditional steel reinforcement, especially in harsh environments on bridges, outside garages and off-shore structures. The GFRP bars are very different from steel, mainly due to much lower elasticity modulus and their anisotropic structure. Good performance of FRP reinforced concrete requires adequate interfacial bond between bars and concrete, mainly due to surface preparation. The authors' own experimental program includes twelve beam bond tests carried out on rectangular beams consisted of two concrete blocks connected by a continuous GFRP bar in tension and by a steel hinge in compression. Two main parameters were investigated in the tests: bar diameter and thickness of a bottom concrete cover. The GFRP bars indicated good bond behavior to concrete, mainly due to the ribs on the bar surface. The results of the test indicated the decrease in the ultimate shear bond stress with the increase in the bar diameter regardless of the thickness of the concrete cover. The decrease in the concrete cover caused the decrease in the shear bond stress for all bars diameters. The increase in bar diameter caused the decrease in the ultimate bond strength.

© 2017 The Authors. Published by Elsevier Ltd. This is an open access article under the CC BY-NC-ND license (<http://creativecommons.org/licenses/by-nc-nd/4.0/>).

Peer-review under responsibility of the scientific committee of the International Conference on Analytical Models and New Concepts in Concrete and Masonry Structures

**Keywords:** Bond; GRFP bar; beam test; failure; ultimate shear strength; slip

---

\* Corresponding author.

E-mail address: [renata.kotynia@p.lodz.pl](mailto:renata.kotynia@p.lodz.pl)

## 1. Introduction

Fiber reinforced polymer (FRP) reinforcement has been increasingly used as a replacement for traditional steel reinforcement in reinforced concrete (RC) structures for the last decade. FRP reinforcement is currently competitive resistance, good non-magnetic properties, and very good fatigue resistance. The most popular kind of FRP reinforcement is that made of glass fiber reinforced polymer (GFRP), which is cheaper than other FRP bars. The GFRP bars are very different from steel, mainly due to their much lower elasticity modulus and bond to concrete behavior that is highly effected by preparation of the surface.

Good performance of FRP reinforced concrete requires adequate interfacial bond between bars and concrete, due to the tensile stress transfer from concrete matrix to reinforcement. Bond-slip interaction between the FRP bar and surrounding concrete is ensured by the stress propagation which depends on bar's geometry, mechanical interaction, chemical adhesion and frictional forces as well as the compressive strength of concrete. The following parameters have the main effect on the bond behavior of the FRP reinforcement to concrete: the nominal diameter of bars, concrete cover, the type of FRP bar, its surface preparation, bond length, and concrete strength. All these parameters have been analyzed and discussed in the paper.

The review of the existing research on the FRP-to-concrete bond behavior has shown that contrary to conventional steel bars, a GFRP bar has no standardization for surface preparation. Variable surface characteristics based on: a sand-coated, ribbed surface with rope winding, a helically wrapped surface, an indented and wrapped GFRP bar, strongly affect the bond behavior between GFRP and concrete.

There is a lot of research on bond behavior of FRP reinforcement to concrete based mainly on: the direct pull-out test, the beam test, the splice test and the ring pullout test [1-8]. The setups of direct and ring pullout test do not correspond to the real bond conditions existing in a reinforced concrete element. Hence, only the beam test and splice test can reflect the real evaluation of the reinforcement bond behavior.

There is not many research on the beam bond tests with FRP reinforcement [7, 8, 9]. Selected studies of the bond tests are summarized in Table 1 with corresponding investigated parameters.

Table 1. Existing bond test models.

Type of research	$\phi$ [mm]	$L_b$	Investigated parameters			Reference
			FRP type	$a/c$ [mm]	various surface	
Pull out test	8,9,10,12,13,16,19,20	$4\phi, 5\phi, 10\phi$	GFRP,CFRP	75, 100	✓	[1], [2], [3], [4], [5], [6]
Beam test	8,12,16,20	$5\phi, 6\phi, 10\phi, 16\phi, 20\phi$	GFRP	15, 30	✓	[7], [8], [9]

The best method to determine the bond behavior seems to be the bending method, because it considers the actual operating conditions of a structural element. The investigated parameters considered in the beam bond are presented and compared according to variables in Table 2. The analysis of the existing studies has become the main contribution to the authors' own research on the beam bond test to investigate the bond behavior of the GFRP bars to the concrete. The GFRP bars indicated good bond behavior in all the analyzed research. In the majority of studies the specimens failed by debonding of the bars from concrete, indicating that the bond length to attain the ultimate tensile strength of the FRP bars is higher than  $20\phi$  [7, 9].

Table 2. Investigated parameters in existing beam bond tests.

Reference	Nominal diameter	Embedment length	Concrete cover	Rebar surface treatment	Failure mode type
H. Mazaheripour, J.A.O. Barros [6]	✓	✓	✓	✓	✓
Tighiouart B, Benmokrane B [7]	✓	✓		✓	✓
Pecce M, Manfredi G [8]		✓			✓

The ultimate bond stress of the bar ( $\tau_u$ ) can be defined as an average bond shear stress over the embedded length, and can be calculated with the following equation:

$$\tau_u = \frac{F_u}{\pi \cdot \phi \cdot L_b}, \quad (1)$$

where  $F_u$  is the pull-out force,  $\phi$  is a nominal bar diameter and  $L_b$  is the embedded bond length.

A type of the bar surface had the most significant influence on the bond behavior [7]. GFRP bars showed lower shear bond stress than steel bars with the same diameter [8]. The ribs in GFRP bars were superficially sheared off, which confirms that bond behavior strongly depends on the concrete strength of the bar ribs. The increase in a slip loaded end  $s_{lp}$  and the bond length  $L_b$  is more pronounced in the ribbed bars than in the sand coated bars [7]. Moreover, the ribbed bars have a higher bond stiffness and the bond shear stress than the sand-coated bars [8]. An increase in the bar diameter caused a decrease in the shear bond stress and a decrease in the ultimate bar slip.

## 2. Experimental program

### 2.1. Test specimens

The aim of the tests was to determine the bond behavior of GFRP bars to concrete on the beam bond setup. A test program contained twelve rectangular concrete beams with a cross section of 150 x 200mm specimens with the length of 800mm (Fig. 1). The beams used in the tests consisted of two concrete blocks connected to each other by FRP reinforcement in tension and by a steel hinge in compression. Two main parameters were investigated in the tests: the diameter of GFRP bars (12mm, 16mm, 18mm) and the thickness of the bottom concrete cover (15mm and 35mm). Each type of the beam was duplicated in order to collect double test results. The summary of the tested elements is shown in Table 3. The thickness of the concrete cover and the bar diameter varied in order to investigate their influence on the GFRP to concrete bond behavior. The embedment length for all specimens was assumed to be 10 times of bar diameters ( $10\phi$ ). In the front part of each block, the bar was unbonded on the length of 50 mm to avoid premature fracture of concrete in the edge zone. The embedment length was only changed in the tested block, while in the opposite the block the full embedment length of 335 mm was tested in all specimens. The steel stirrups of 6mm diameter at a spacing of 100mm were used to avoid the shear failure (see Fig. 1a). The top reinforcement consisted of two steel bars with 10mm diameter. The beam's nomenclature consists of: bars diameter; bond length in mm (e.g. L120); the concrete cover thickness in mm and the finally is beam's number from two beams with the same configurations.

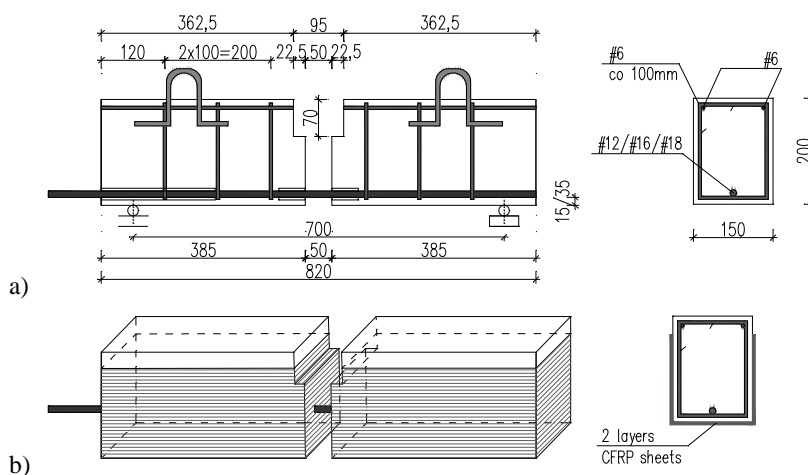


Fig. 1. Reinforcement of beams and additional 2 layers of CFRP strengthening (lateral and bottom fibres in horizontal direction).

Due to the lack of additional longitudinal reinforcement in the test beam block, concrete cracking occurred at the end of the bond length in two first tested specimens: 12-L120-15.1 and 12-L120-15.2. In order to avoid this cracking in next two beams 18-L180-15.1 and 16-L160-35.1 externally bonded carbon fiber reinforced polymer (CFRP) sheets were applied on the bottom side of the concrete blocks in longitudinal direction (2 layers of 0.13 mm thickness). As this bottom strengthening was still ineffective and did not prevent the concrete from cracking at the end of the bond length, additional lateral strengthening besides the bottom one was applied on the concrete blocks in a longitudinal direction (2 layers of 0.13 mm thickness, see Fig. 1b). This external strengthening of each concrete block made the fully wrapped horizontal confinement and efficiently improved the bond behavior of the internal GFRP bar in concrete. For the other elements, failure of ribs due to their pulling on the GFRP bars surface appeared, which confirmed the bond loss. It should be noted that the members which failed due to concrete cracking (12-L120-15.1, 12-L120-15.2, 18-L180-15.1 and 16-L160-35.1) will not be further considered in the analysis of test results.

Table 3. Configuration of tested beams.

Elements	Bottom reinforcement		Top reinforcement		Stirrups	Concrete cover [mm]	Bond length [mm]
	$\phi$ [mm]	A [mm <sup>2</sup> ]	$\phi$ [mm]	A [mm <sup>2</sup> ]			
12-L120-15.1	12	113	6	57		15	120
12-L120-15.2	12	113	6	57		15	120
16-L160-15.1	16	201	6	57		15	160
16-L160-15.2	16	201	6	57		15	160
18-L180-15.1	18	254	6	57		15	180
18-L180-15.2	18	254	6	57	$\phi 6$ at spacing 100 mm	15	180
12-L120-35.1	12	113	6	57		35	120
12-L120-35.2	12	113	6	57		35	120
16-L160-35.1	16	201	6	57		35	160
16-L160-35.2	16	201	6	57		35	160
18-L180-35.1	18	254	6	57		35	180
18-L180-35.2	18	254	6	57		35	180

## 2.2. Material characteristics

The GFRP bars with single braid ribs shown in Figure 2 were tested in tension. The tensile strength obtained in test was 1109 MPa, 1205 MPa and 1281 MPa for the bars of 18mm, 16mm and 12mm diameter, respectively. The average value of the modulus of elasticity was equal of 50.5 GPa. The compressive strength along the fibres declared by the producer was adopted as not lower than 350 MPa. The spacing ribs of bars ranged from 6.8 mm to 8.5 mm for 18mm bar diameter and from 7.5mm to 9.6mm for 12 mm bar diameter, that was no significant impact on the GFRP-to-concrete bond behavior and the final test results.

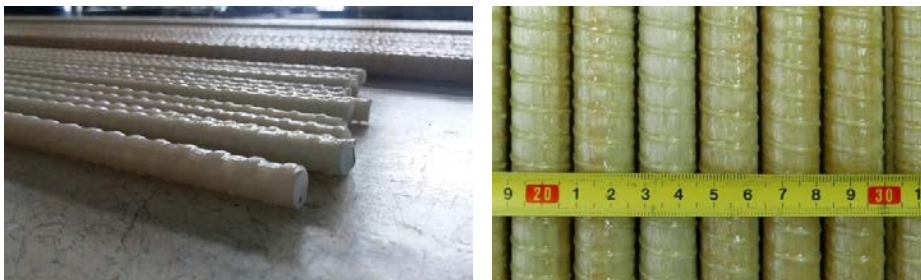


Fig. 2. GFRP bars used in the test.

The concrete mix was made of sand, crushed stone and cement CEM I 42.5 with the addition of a plasticizer. The concrete mix is composed of: sand 0/2 – 970 kg/m<sup>3</sup>, crushed stone 2/8 – 860 kg/m<sup>3</sup>, water – 205 kg/m<sup>3</sup>, CEM I 42,5 Rudniki CEMEX – 255 kg/m<sup>3</sup>, plasticizer BV- Cemex Admixtures – 1,8 kg/m. The experimental compressive concrete strength ranged from 34.3 MPa to 36.3 MPa with an average value of 35.4 MPa (COV=2.65%). The detailed results of concrete tests are summarized in Table 4.

### 2.3. Test setup and measurements

The test setup consisted of: a steel frame made of plate girders, a hydraulic jack attached to the upper girder, a device supplying the servo-motor and steel hinged supports (Fig. 3). The beams were tested in the four point loaded set-up by the displacement control system with the hydraulic jack of 200kN capacity shown in Fig. 3. The load was applied monotonically with a velocity of 10μm/s.

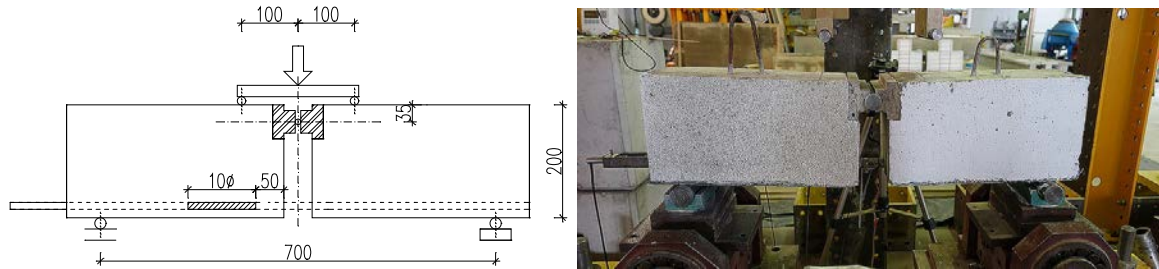


Fig. 3. Test set up.

The system of measuring devices consisted of linear variable differential transducers (LVDT) and one strain gauge installed on the bar surface at the specimen symmetry axis to record the bar slip of the FRP bar in reference of the central beam's edge, while LVDT 4 was fixed to the free bar end and measured the relative slip between the free bar end and the outer beam's edge. Two horizontal LVDTs No 2 and 3 were applied along the embedded bar length to measure concrete strain at both ends of the bond length of the bar (see detail in Fig. 4). All readings were continuously recorded every one second.

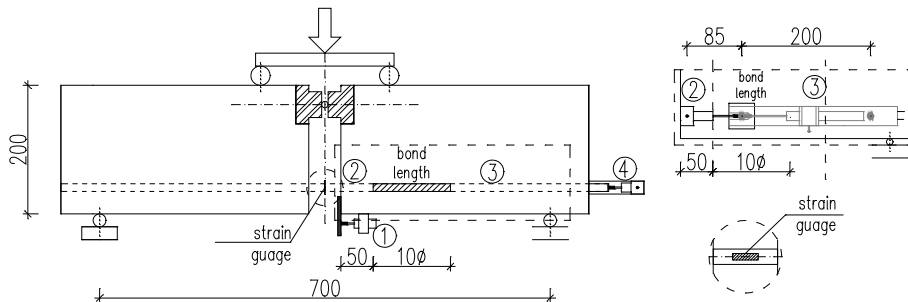


Fig. 4. Scheme of measurements.

## 3. The analysis of test results

### 3.1. Experimental results

Beams 12-L120-15.1 and 12-L120-15.2 as well as the strengthened ones 18-L180-15.1 and 16-L160-35.1, which failed due to concrete cracking were removed from the analysis of the test results. The other members strengthened with horizontal and bottom confinement with two CFRP sheet layers failed due to GFRP bars pulling from the embedded concrete, which confirmed the bond loss of the bar to the concrete. Bond failure developed partially along

the surface of the bars and partially in the surrounding concrete by peeling off the external fibres of the bar. Failure mode was most often caused by splitting of the ribs along the GFRP bars. This failure developed with the gradual damage of the bar ribs pulling from the bar surface along the bond length. A concrete cover of each specimen test block was cut and removed after testing in order to make clear verification of the failure mode along the bond length. Fig. 5 shows examples of bare bars with partially splitted ribs after removal of the concrete cover.

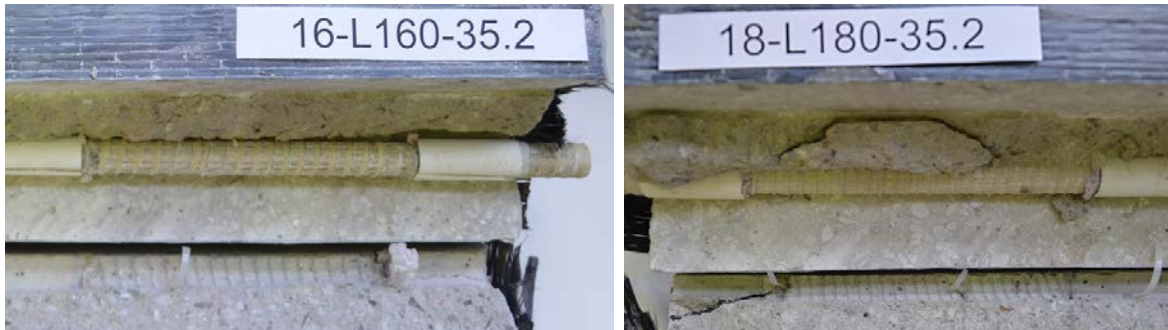


Fig. 5. Failure of the ribs along the bar embedded length in specimens (a) 16-L160-35.2, and (b) 18-L180-35.1.

Based on the ultimate load that led to the bar bond failure ( $F_u$ ) the tensile force in the bar ( $F_b$ ) was calculated from the equilibrium between the applied load, corresponding reactions, and the arm of internal forces. All test results with values of the loaded and free bar end slip for the ultimate loads ( $s_{lp}$ ,  $s_{fp}$ ) are shown in Table 4.

Table 4. Test results.

Elements	$\phi$ [mm]	$f_c$ [MPa]	$f_{cr}$ [MPa]	$F_u$ [kN]	$F_b$ [kN]	$s_{lp}$ [mm]	$s_{fp}$ [mm]	$\tau_u$ [MPa]	Failure mode
12-L120-15.1	12	35.9	3.65	-	-	-	-	-	cracking
12-L120-15.2	12	35.9	3.65	-	-	-	-	-	cracking
16-L160-15.1	16	34.3	3.10	69.34	61.04	1.23	0.29	7.59	ribs failure
16-L160-15.2	16	36.3	3.00	70.49	62.05	1.27	0.91	7.72	ribs failure
18-L180-15.1	18	36.3	3.00	80.42	-	-	-	-	cracking
18-L180-15.2	18	36.3	3.00	71.65	63.46	-	0.17	6.24	ribs failure
12-L120-35.1	12	36.3	3.00	49.59	49.99	2.61	0.71	11.05	ribs failure
12-L120-35.2	12	34.3	3.10	54.33	54.77	3.42	0.93	12.11	ribs failure
16-L160-35.1	16	36.3	3.00	71.78	73.55	2.08	0.52	9.15	ribs failure
16-L160-35.2	16	34.3	3.10	70.84	-	-	-	-	cracking
18-L180-35.1	18	34.3	3.10	75.90	78.33	2.59	0.56	7.70	ribs failure
18-L180-35.2	18	34.3	3.10	72.55	74.84	0.53	0.62	7.36	ribs failure

Test results indicated that the increase in the bar diameter caused the decrease in the free bar end slip corresponding to the ultimate shear bond stress ( $\tau_u$ ) (Fig. 6). The increase in the bar diameter caused the decrease in the ultimate shear bond stress in both cases of the concrete cover (35 mm and 15 mm). The increase in the bar diameter from 16 mm to 18 mm confirmed the decrease in the ultimate shear bond stress ( $\tau_u$ ) by 22% and 18% for a thickness of concrete cover of 35 mm and 15 mm respectively. The increase in the bar diameter from 12 mm to 16 mm caused the decrease in the ultimate shear bond stress by about 21% for a thickness of concrete cover of 35 mm. The reason of the decrease was a longer bond length and a greater contact surface of the bar and the surrounding concrete. Moreover a higher bar diameter caused the bond failure faster and more brittle. The increase in the bar diameter from 12 mm to 16 mm led to the decrease in the free bar end slip ( $s_{fp}$ ) over 36% for a concrete cover

thickness of 35 mm. The increase in bar diameter from 16 mm to 18 mm caused the decrease in the free bar end slip over 71% for a concrete cover thickness of 15 mm, contrary to beam with the thickness of concrete cover of 35 mm.

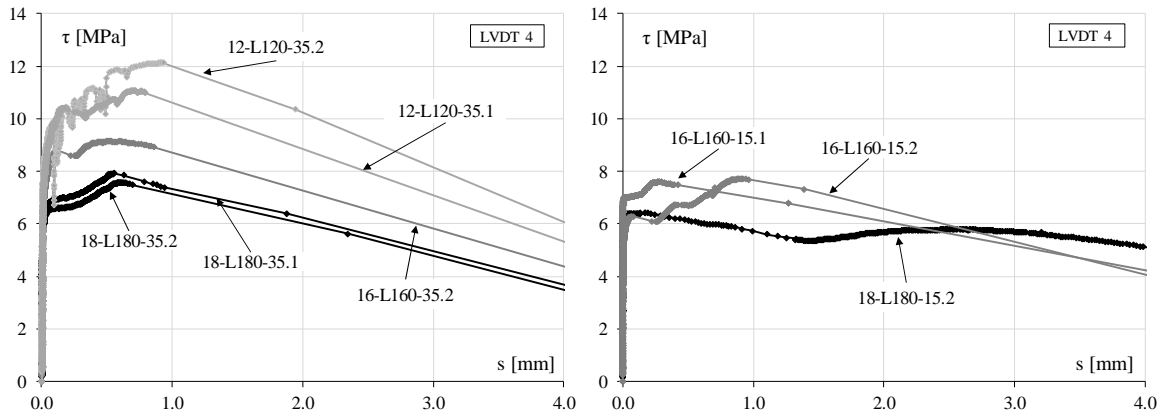


Fig. 6. Free end slip-shear bond stress plots: (a) for 35 mm concrete cover (b) for 15 mm concrete cover.

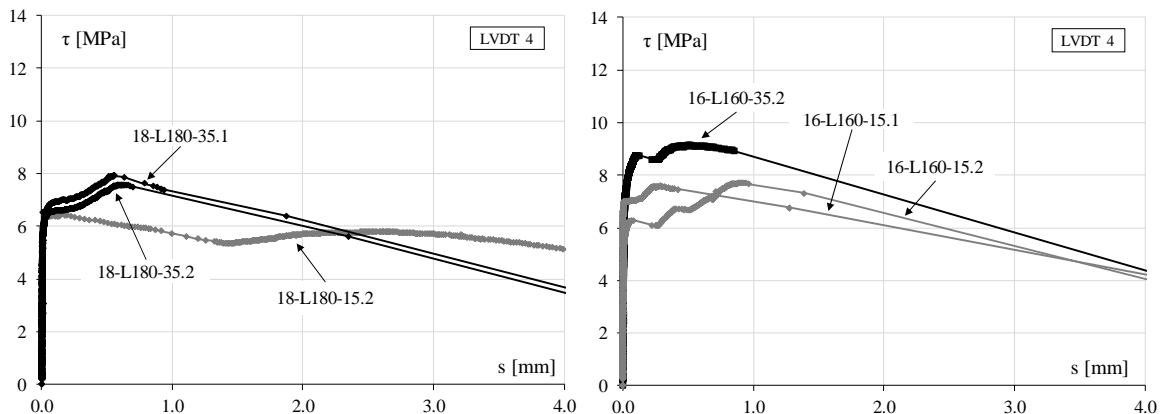


Fig. 7. Comparison of the free slip-shear bond stress plots for bars: (a) 16mm diameter, (b) 18mm diameter.

The increase in the concrete cover thickness from 15 mm to 35 mm led to the increase in the ultimate shear bond stress and the increase in the free end slip corresponding to the ultimate shear bond stress. Generally, the decrease in the concrete cover led to the decrease in the tensile stress in the surrounding concrete transferred into the bar and finally led to the significantly brittle failure (compare Fig. 6a and 6b). The increase in the concrete cover thickness by 20 mm caused the increase in the ultimate shear bond stress ( $\tau_u$ ) by 19% and 21% for a diameter of bars of 16 mm and 18 mm respectively (compare Fig. 7).

There was not observed bar debonding or tensile failure of the bar, which confirmed that the bond length equal of 10 times of the bar diameters was suitable bond length.

The test results are comparable to those from studies [7] obtained for the same bond length  $L_b$  and the similar compressive concrete strength. Differences in the ultimate shear bond stresses between authors' own research and studies [7] equal of 6%, 2% and 12% for the bar diameters of 12mm, 16mm and 18mm, respectively.

The beam bond tests will be continued with higher concrete strength (C50/60) in order to investigate an effect of the concrete strength on the GFRP to concrete bond behavior. The all tests results will be used for calibration of the bond-slip model for the GFRP bars used in the research.

#### 4. Conclusions

Beam bond tests carried out on twelve concrete specimens enabled to draw the following conclusions:

- the GFRP bars indicated good bond behavior to concrete, mainly due to the ribs on the bar surface;
- the increase in the bar diameter caused the decrease in the shear bond stress in both cases of the concrete cover thickness;
- the increase in the bar diameter from 16 mm to 18 mm indicated the decrease in the ultimate shear bond stress ( $\tau_u$ ) by 22% and 18% for the thickness of concrete cover of 35 mm and 15 mm, respectively;
- the increase in the bar diameter led to the decrease in the slip free ends ( $s_{fp}$ ) corresponding to the ultimate shear stress;
- the increase in the compressive concrete strength caused much better bar-to concrete bond behavior;
- the decrease in the concrete cover thickness led to the decrease in the shear bond stress in both cases of the bar diameter.

#### Acknowledgements:

The authors gratefully acknowledge the ComRebars Company who supplied the GFRP reinforcement for the experimental tests.

#### References

- [1] M. Baena, L. Torres, A. Turon, C. Barris, Experimental study of bond behaviour between concrete and FRP bars using a pull-out test, *Composites: Part B* 2009;40(8), 784–97.
- [2] F. AL-Mahmoud, A. Castel, R. Francois, C. Tourneur, Effect of surface preconditioning on bond of carbon fiber reinforced polymer rods to concrete, *Cement & Concrete Composites* 2007;29(9), 677–89.
- [3] J.Y. Lee, T.Y. Kim, T.J. Kim, C.K. Yi, J.S. Park, Y.C. You, et al, Interfacial bond strength of glass fiber reinforced polymer bars in high-strength concrete, *Composites: Part B* 2008;39(2), 258–70.
- [4] Q. Hao, Y. Wang, Z. He, J. Ou. Bond strength of glass fiber reinforced polymer ribbed rebars in normal strength concrete. *Construction Build Mater* 2009;23(2), 865–71.
- [5] W. Jong-Pil, P. Chan-Gi, K. Hwang-Hee, L. Sang-Woo, J. Chang-II, Effect of fibers on the bonds between FRP reinforcing bars and high-strength concrete, *Composites Part B: Engineering*, Volume 39, Issue 5, July 2008, 747-755.
- [6] M. Do-Young, S. Jongsung, O. Hongseob, Experimental characterization of the bond performance of a new type of glass fibre-reinforced polymer rebar for application in concrete structures, *Journal of Materials Design and Applications* 221(2): April 2007, 113-119.
- [7] H. Mazaheripour, J.A.O. Barros, J.M. Sena-Cruz, M. Pepe, E. Martinelli, Experimental study on bond performance of GFRP bars in self-compacting steel fiber reinforced concrete, *Composite Structure*, 95 (2013), 202-212.
- [8] B. Tighiouart, B. Benmokrane, D. Gao, Investigation of bond in concrete member with fiber reinforced polymer (FRP) bars, *Constr Build Mater*. 1998;12(8), 453–62.
- [9] M. Pecce, G. Manfredi, R. Realfonzo, E. Cosenza, Experimental and analytical evaluation of bond properties of GFRP bars, *Journal of Materials in Civil Engineering* 2001;13(4), 282–90.